J. Quant. Spectrosc. Radiat. Transfer Vol. 30, No. 1, pp. 37–44, 1983
Printed in Great Britain.

0022-4073/83/070037-08$03.00/0
Pergamon Press Ltd.

INFRARED ABSORPTION INTENSITIES OF NITROUS ACID (HONO) FUNDAMENTAL BANDS

ROBERT H. KAGANN† and ARTHUR G. MAKI
National Bureau of Standards, Washington, DC 20234, U.S.A.

(*Received* 30 *June* 1982)

Abstract—A Fourier transform spectrometer with a resolution of 0.06 cm^{-1} was used to measure the absorption intensities of the four in-plane fundamental bands (ν_1, ν_2, ν_3 and ν_4) of *trans*-nitrous acid (HONO) and three of the in-plane fundamental bands (ν_1, ν_2 and ν_4) of *cis*-nitrous acid. The equilibrium constants for the reactions $NO + NO_2 + H_2O \rightleftarrows 2HONO$, $NO + NO_2 \rightleftarrows N_2O_3$, and $2NO_2 \rightleftarrows N_2O_4$ were used to determine the partial pressure of HONO in the gas mixture in the absorption cell. Interferences from overlapping absorptions of NO_2, H_2O and other species were digitally subtracted from the spectra.

1. INTRODUCTION

Because of the need to understand the details of the chemistry of the upper atmosphere, there has been much interest in measuring ambient atmospheric concentrations of the various oxides and hydrogen oxides of nitrogen. The chemistry of these species is complex and there is evidence that the formation of nitrous acid, HONO, in the atmosphere is too slow for equilibrium to be established.[1,2] Under these circumstances, the role of HONO can be best understood if the concentration is determined through spectroscopic observations. There are, however, no values in the literature of absolute intensities of the HONO absorption bands. The present work was undertaken to provide absolute intensity measurements for the major absorption bands of HONO at frequencies greater than 700 cm^{-1}.

At room temperature, it is impossible to obtain a pure gas phase sample of HONO since it disproportionates to form an equilibrium mixture of NO, NO_2 and H_2O. Further reactions among disproportionation products result in small quantities of N_2O_3, N_2O_4, and HNO_3 in the mixture. In addition, HONO which is a planar molecule, exists in two isomeric forms (*cis* and *trans*) and these are also in equilibrium at room temperature.

Jones *et al.*[3] and McGraw *et al.*[4] studied the infrared spectra and made vibrational assignments of *cis*- and *trans*-nitrous acid. They located the four in-plane vibrational fundamental bands at roughly 3500, 1700, 1250, and 850 cm^{-1}. The two out-of-plane modes for both tautomers are at lower frequencies. From the study of the spectrum at different temperatures, Jones *et al.*[3] determined that the *trans*-tautomer is lower in energy than the *cis* by 177 ± 87 cm^{-1} and, similarly, McGraw *et al.*[4] determined an energy difference of 186 ± 350 cm^{-1}. Varma and Curl[5] have obtained a more accurate estimate of 141 ± 35 cm^{-1} for this energy difference.

More recently, laser-Stark measurements have been made on the 1700 and 1640 cm^{-1} ν_2 fundamental bands of *trans*- and *cis*-HONO, respectively.[6] These measurements have provided upper and lower state rotational constants for these vibrational bands, which verify the *trans*- and *cis*-assignments made in Refs. 3 and 4. High-resolution tunable diode laser measurements have also been made[7] on the ν_2 band of *trans*-HONO and the ν_4 band of *cis*-HONO, again verifying the *cis*-*trans* assignments for the ν_2 and ν_4 bands. Chan *et al.*[2] have used Fourier transform spectroscopy to study the rate of formation of HONO from a very low concentration mixture of H_2O, and NO_2, and NO in air. They used lower spectral resolution than we and were primarily interested in the relative time dependence of the intensities at the 1263 and 852 cm^{-1} Q-branch maxima.

2. EXPERIMENTAL DETAILS

We formed HONO by mixing measured amounts of NO, NO_2, and gaseous H_2O in a one liter gas mixing vessel, fitted with a cold finger and a teflon stopcock. The mixing vessel was

†Present address: CODE 913, NASA Goddard Space Flight Center, Greenbelt, MD, U.S.A.

attached to a glass manifold which in turn was open to a capacitance manometer (calibrated at the National Bureau of Standards). The manifold volume was ~ 500 mL. The mixing and pressure measurement procedures were as follows: we introduced NO_2 to the mixing vessel (opened to the manifold) and measured the pressure. The NO_2, in the mixing vessel and the manifold, was transferred (by way of condensation at liquid nitrogen temperature) to a small volume (~ 10 mL) storage cold finger attached to the manifold and isolated by a teflon stopcock. After the storage cold-finger stopcock was closed, H_2O vapor was introduced into the manifold and mixing vessel and the pressure was measured and recorded. Gas-phase H_2O was transferred to the storage cold finger, where it was condensed on top of the frozen NO_2. The storage cold finger stopcock was closed and NO was introduced into the manifold and mixing vessel. The pressure of the NO was measured and recorded, then the NO was condensed in the mixing vessel cold finger. The stopcock to the storage finger was opened and the frozen NO_2 and H_2O were warmed, resulting in condensation of the $H_2O + NO_2$ mixture on top of the frozen NO in the mixing vessel. When the transfer to the mixing vessel was complete, the mixing vessel was closed to the manifold and the frozen mixture was allowed to warm and form the gas phase equilibrium mixture. After equilibrium took place, the manifold and then the absorption cell were filled with the mixture and the new equilibrium pressure was measured and recorded. Ideally, this pressure should be equal to the sum of the pressures measured for the individual gases plus stoichiometric changes due to the production of HONO and N_2O_3.

We made HONO intensity measurements of the spectra of five different HONO equilibrium mixtures. The overall pressure of these mixtures was ~8000 Pa (60 torr). The composition of the mixtures covered the following ranges: 82–88% NO, 5–9% NO_2, 5–9% H_2O, and 1–2% HONO. The actual partial pressures used are given in Table 1. Since the NO absorption bands do not overlap the HONO absorption bands, a large excess of NO was used for all of the measurements in order to maximize the amount of HONO and minimize the amount of NO_2 and H_2O.

The 19.90-cm gas cell was fitted with BaF_2 windows which were measured to be parallel to within 0.1% of the pathlength. Although the BaF_2 windows are opaque below 700 cm^{-1}, we chose this material because it is relatively impervious to chemical attack by any of the components of the gas mixture. Nevertheless, the windows of the absorption cell slowly developed an absorption band near 1350 cm^{-1} over a period of several weeks, thus indicating a slow reaction with the gases. The spectrum of a HONO mixture gas sample held in the absorption cell for three hours was unchanged from the spectrum of the same sample taken about 30 min after filling the cell.

The spectra were measured with a commercially available Fourier transform spectrometer (FTS) of conventional design with an optimum resolution of 0.06 cm^{-1}. All the spectra were unapodized and obtained at the maximum resolution. The spectrum obtained in each of the five runs involved two hours of signal averaging (512 mirror sweeps). Each of the five spectra was digitally divided by 4-hr (1024 mirror sweeps) background spectrum of the evacuated gas cell to obtain a transmittance ($T = I/I_0$) spectrum.

Table 1. Calculated partial pressures of the constituents in the equilibrium mixtures, corrected to 296 K, all pressures are in torr.

Run	P_{NO}	P_{NO_2}	P_{H_2O}	$P_{trans\text{-}HONO}$	$P_{cis\text{-}HONO}$	$P_{N_2O_3}$	$P_{N_2O_4}$
1	53.82	2.99	4.02	0.667	0.336	0.105	0.075
2	49.40	5.10	3.94	0.870	0.438	0.185	0.262
3	50.92	5.09	4.07	0.872	0.440	0.180	0.238
4	46.86	4.74	3.76	0.777	0.391	0.154	0.206
5	52.15	3.67	5.18	0.849	0.427	0.133	0.125

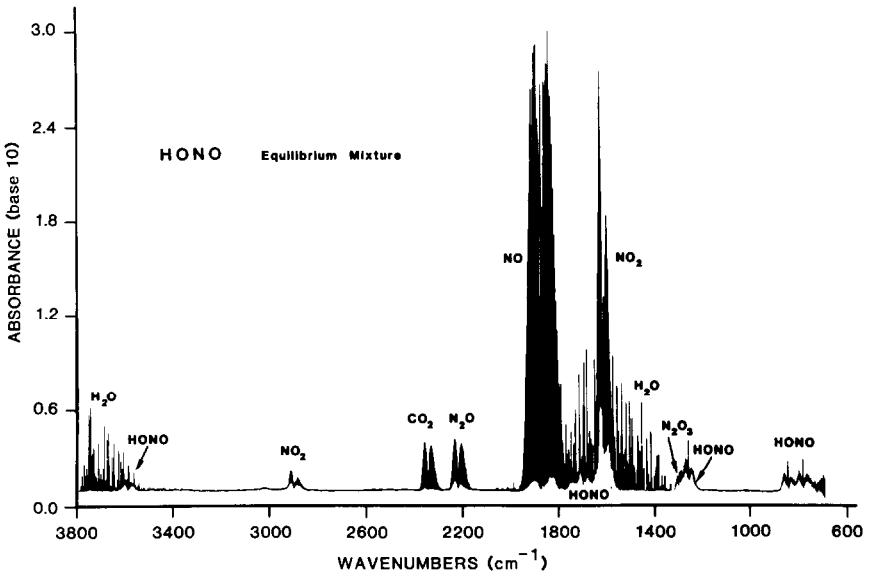

Fig. 1. Spectrum of the equilibrium mixture in Run 1. See Table 1 for the partial pressures of the components.

After the HONO mixture was introduced into the gas cell, about 10^5 Pa (760 torr) of 99.999% N_2 gas was added to pressure-broaden the rovibrational lines to minimize instrument distortion due to the 0.06 cm^{-1} resolution. Since the measurements all involved low partial pressures of HONO, the measured absorption due to HONO was generally less than 40%. The limited range of pressure-pathlength products available for this work made it difficult to interpret a Beer law plot for saturation effects arising from insufficient instrumental resolution. Nevertheless, errors from such effects must be small since we find that measurements made on NO(1–0), $N_2O(\nu_1)$ and $OCS(\nu_1)$ under the same experimental conditions gave values for the band strengths which agreed with the literature values[8,9] to within 2, 4, and 0.3%, respectively. In the first two cases, the values were slightly larger than our estimates of the best literature values, whereas errors due to insufficient instrumental resolution would give values that were too small.

As can be seen in Fig. 1, some of the absorption bands of HONO were severely overlapped by the absorption bands due to the various other molecules present in the mixture. A spectrum of a pure gas sample of each entering species† was digitally subtracted from the spectrum of the HONO mixture in order to obtain the spectrum of pure HONO (see Figs. 2–4). This spectrum of HONO, which was digitally purged of interfering absorption, was used to determine the integrated absorption of the HONO bands.

To obtain the integrated intensities, the bands were plotted as absorbance $A(\nu)$ vs wavenumber ν, where

$$A(\nu) = -\ln [I(\nu)/I_0(\nu)]. \tag{1}$$

According to the Beer–Lambert law,

$$A(\nu) = k(\nu)pl, \tag{2}$$

where $k(\nu)$ is the absorption coefficient, P is the pressure, and l is the pathlength through the absorbing species. The band strength S is defined as

$$S = \int_{\text{band}} k(\nu)\, d\nu \tag{3a}$$

†In the case of the overlapping N_2O_3 ν_3-band, a spectrum of N_2O_3 was obtained by digitally subtracting the NO, NO_2, and N_2O_4 spectra from the spectrum of an equilibrium mixture of NO, NO_2, N_2O_4.

or

$$S = \int_{\text{band}} A(\nu)\, d\nu / Pl. \tag{3b}$$

We obtained values for $\int_{\text{band}} A(\nu)\, d\nu$, both by digital integreation of the absorption band and by graphically measuring the area under the curve. The graphical method was preferred because of the greater ease and flexibility in dealing with artifacts such as changing background I_0 or incomplete elimination of interfering absorption due to H_2O, NO_2 and other species.

3. THE GAS-PHASE EQUILIBRIUM SYSTEM

After pure gas samples of NO, NO_2, and H_2O were introduced into the absorption cell, a complex equilibrium system was established which follows the equilibrium equations

$$NO + NO_2 + H_2O \rightleftarrows 2HONO, \tag{4}$$

$$2NO_2 \rightleftarrows N_2O_4, \tag{5}$$

$$NO + NO_2 \rightleftarrows N_2O_3, \tag{6}$$

$$3NO_2 + H_2O \rightleftarrows 2HNO_3 + NO. \tag{7}$$

Although some of these reactions, notably those in Eq. (4), may be very slow under certain conditions, measurements made several hours apart indicate that, under our experimental conditions, all significant equilibria were established before the spectroscopic measurements of each mixture were made.

Our spectra clearly showed the spectral features of N_2O_4 and N_2O_3, but the concentration of HNO_3 was too low for observation of absorption bands in our samples. The result is consistent with the concentrations calculated from the equilibrium constants reported in Refs. 10–15. The absence of HNO_3 resulted from the use of equilibrium mixtures containing a large proportion of NO, which forced the equilibrium of Eq. (7) to the left, thus inhibiting formation of HNO_3. This is a particularly important point since the absorption bands of HNO_3 are strong and severely overlap the HONO bands. High resolution diode laser measurements[7] verified the complete absence of interference from HNO_3 in the mixtures studies in the present work.

To determine the concentrations of HONO in a given sample, it was necessary to solve the simultaneous equations,

$$K_1 = \frac{[HONO]^2}{[NO][NO_2][H_2O]} = 1.36\ \text{atm}^{-1}, \tag{8}$$

$$K_2 = \frac{[N_2O_3]}{[NO][NO_2]} = 0.59\ \text{atm}^{-1}, \tag{9}$$

$$K_3 = \frac{[N_2O_4]}{[NO_2]^2} = 8.1\ \text{atm}^{-1}, \tag{10}$$

where the values of the equilibrium constants K_1, K_2, and K_3 were taken from Refs. 11, 15, and 13, respectively, at 296 K. In our calculations, we used the initial quantities of NO, NO_2, and H_2O and the usual stoichiometric relations. The equilibrium constants actually used in the calculations differed slightly from the values given above because the measurements were made at slightly different temperatures (between 295 and 300 K), so the temperature dependences of the equilibrium constants were taken into account. Since the inclusion of Eqs. (9) and (10) in the calculations only made small changes in the calculated NO and NO_2 concentrations, we employed an iterative procedure to determine the concentration of HONO in each mixture.

As an alternative procedure for determining the quantity of HONO in the samples, the spectrum of the mixture was used to determine the equilibrium concentrations of NO, NO_2,

and H_2O. It was possible to estimate the quantity of HONO formed in the mixture from the initial concentrations of H_2O, NO, and NO_2, the final equilibrium concentrations of these gases determined spectroscopically, and the equilibrium constants in Eqs. (9) and (10). Since the equilibrium constant for the formation of HONO [Eq. (8)] is small, one must measure small changes in concentration and this procedure did not give very accurate results. Another procedure was to measure the small reduction in the total pressure as known quantities of the three components (NO, NO_2, and H_2O) were mixed.

In all cases, the results were consistent with the values of the equilibrium constants given in Refs. 10–12 and shown here in Eq. (8). We considered the last two procedures less reliable than the first in which we use Eqs. (8–10) with the literature values for the equilibrium constants.[11,13,15]

To calculate the distribution of *cis*- and *trans*-HONO at the temperature of our measurements, we used the value for the *cis*-, *trans*-energy separations obtained by Varma and Curl.[5] They found that the *trans*-isomer was lower in energy by about 404 ± 100 cal/mole. At 296 K, this results in a 33.5% *cis*-HONO and 66.5% *trans*-HONO distribution. The equilibrium concentrations, which we calculated iteratively from Eqs. (8–10) for the 5 mixtures used in the present work, are given in Table 1.

4. RESULTS AND DISCUSSION

We observed and measured 6 relatively strong HONO absorption bands, *trans*-HONO ν_1, ν_2, ν_3, and ν_4 and *cis*-HONO ν_2 and ν_4. Figure 1 shows the spectrum of the equilibrium mixture before digital manipulation to remove the absorption features that are not due to HONO. Figures 2–4 show more detailed spectra of the ν_1, ν_2, and ν_3 regions, respectively. The ν_4-bands, which have only minor overlapping absorptions by the other components, can be seen in Fig. 1 near 800 cm^{-1} and are similar in appearance to ν_2; however, for ν_4, the *cis*-band is on the blue side of the *trans*-band. We also observed 4 relatively weak bands at 1493, 3257, 3372, and 3427 cm^{-1}. These have been previously assigned as *trans*-HONO $2\nu_3$, *cis*-HONO $2\nu_2$, *trans*-HONO $2\nu_2$, and *cis*-HONO ν_1, respectively.[3,4]

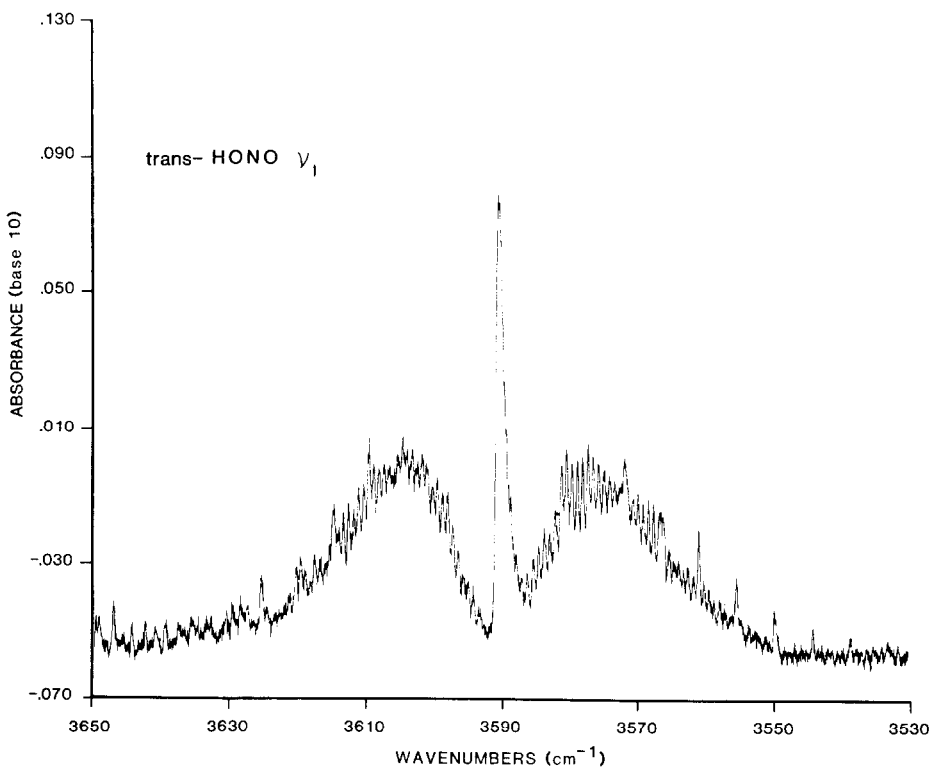

Fig. 2. Spectrum of *trans*-HONO ν_1 with water absorption interferences removed.

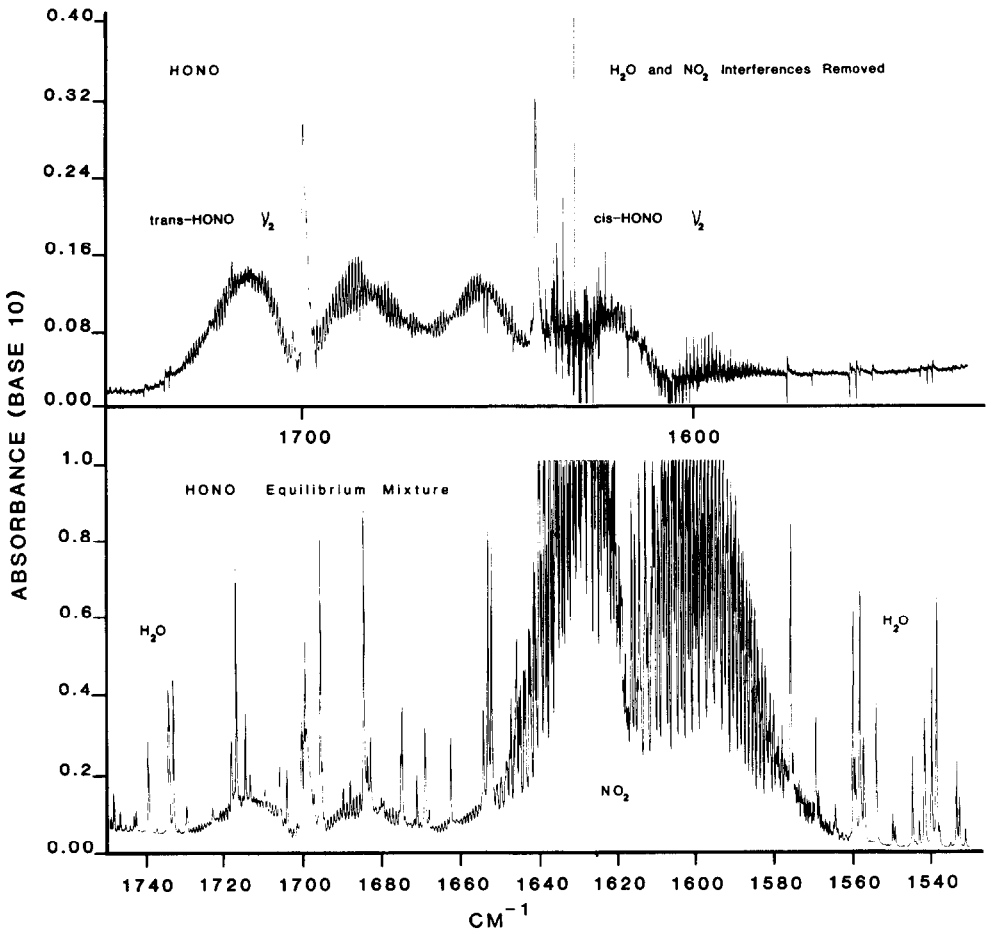

Fig. 3. Spectra of *trans*-HONO ν_2 and *cis*-HONO ν_2. The lower spectrum is the original spectrum of the mixture. The upper spectrum has H_2O and NO_2 absorption interferences removed. Note that the absorbance scale of the upper spectrum is expanded.

We note that the band at 2493 cm^{-1}, with P, Q, and R branches and 32 cm^{-1} separation between the P and R branches, could be assigned to the combination $\nu_2 + \nu_4$ as well as $2\nu_3$. We also note that, with a *trans-cis* population ratio of two to one, the possibility that the band is due to *cis*-HONO cannot be ruled out. The predictions for *cis*-HONO $2\nu_3$ and $\nu_2 + \nu_4$ are only a few wavenumbers from the *trans*-HONO predictions. Unfortunately, we find nothing in our data to help us decide the assignment of this band.

The ν_3 band of *cis*-HONO has not been measured in this work since it is probably much weaker than and buried under the ν_3 band of *trans*-HONO. Because of this possible unresolved overlap, the intensity given for ν_3 of *trans*-HONO may be too large and may represent the sum of the ν_3 bands for both tautomers. Close inspection of Fig. 4 reveals a series of weak Q-branches due to a B-type band on the low frequency side of ν_3. Since the ν_3 bands for both tautomers have both A-type and B-type transitions, it is not certain which tautomer is responsible for these weak B-type transitions.

All of the bands measured in this paper have a toroidal structure that indicates that the A-type transitions dominate the band intensity. As indicated above, weak B-type transitions overlap the ν_3-band of *trans*-HONO. In addition, as can be seen in Fig. 2, the ν_1-band of *trans*-HONO has a significant amount of intensity in B-type transitions that give rise to the series of evenly spaced weak Q-branches spread across the entire band.

Our measured values of the integrated band strengths for the tautomers of HONO are given in Table 2. In the third column are the band strengths (at 296 K) as measured for

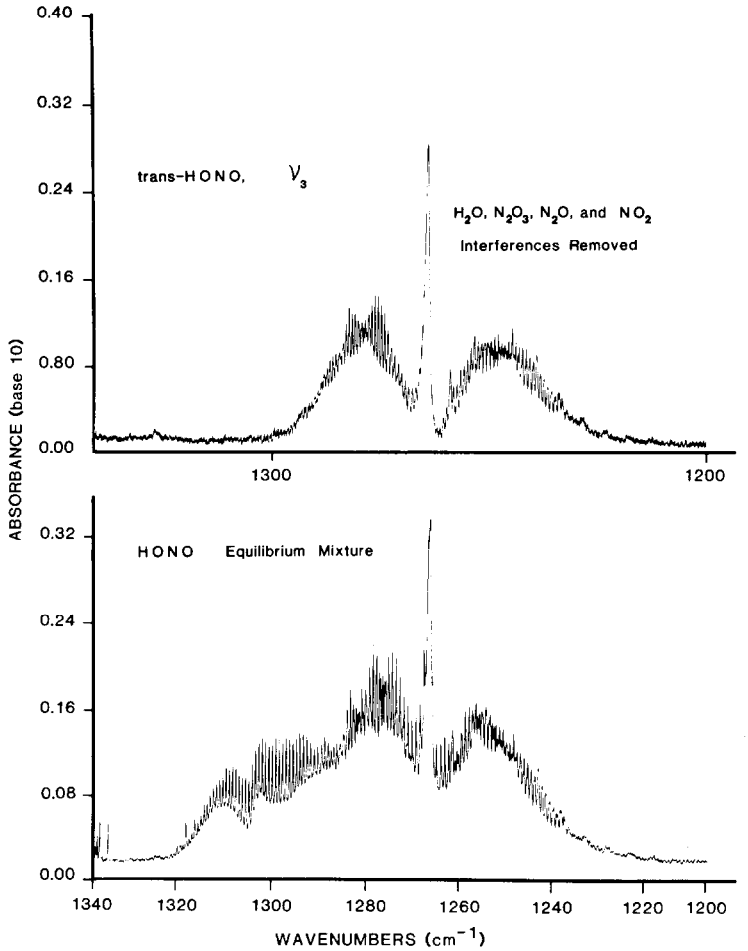

Fig. 4. Spectra for the *trans*-HONO ν_3. The lower spectrum is the original spectrum of the mixture. The upper spectrum has H_2O, N_2O_3, N_2O, and NO_2 absorption interferences removed. In this particular run, N_2O was present as an impurity. Most of the N_2O was removed prior to the subsequent 4 runs.

the equilibrium mixture of the *cis*- and *trans*-isomers. In the fourth column are the strengths (at 296 K) neglecting the *cis-trans* partition, i.e., the pressure P in Eq. (3b) is the total HONO pressure ($P = P_{cis} + P_{trans}$) instead of P_{cis} or P_{trans}. This column allows for easy correction if any of the *cis*-, *trans*-assignments are changed or should a future measurement yield a different value for the *cis-trans* energy separation. The values shown here for the band strengths include a small correction (0.5%) necessary because the infrared radiation is focused at the center of the absorption cell with a divergence angle of 0.14 rad. With our 19.90-cm cell, this results in an effective pathlength of 20.00(10) cm. The uncertainty of 0.10 cm is due mainly to the distribution of pathlengths which the radiation follows and is negligible compared to other sources of error. In the last column in Table 2 are the dipole moment derivatives (or transition moments), $|R_{v''}^{v'}|$, for each vibrational transition. These transition moments were calculated from the band strengths S, viz.

$$S = (8\pi^3 \nu / 3hc)(N'' - N')|R_{v''}^{v'}|^2, \tag{11}$$

where N'' and N' are the number densities for the states v'' and v', respectively.

The uncertainties given in Table 2 were calculated by adding in quadrature the identified uncertainties from different sources and then adding 5% of the value of the band strength to allow for systematic errors.† The identified sources of uncertainty include the

†For the *cis*-ν_1-band, we estimated 25% systematic error because the low signal-to-noise ratio of this band resulted in poor definition of its profile.

Table 2. Measured values of band strengths and dipole moment derivatives of HONO absorption bands.

Band system	Band center, cm^{-1}	Band strength S(296 K), $cm^{-2}atm^{-1}$	Band strength based on total HONO[a] pressure (296 K), $cm^{2}atm^{-1}$	$R_{v''}^{v'}$ debyes[b]
trans ν_1	3590	246(29)[c]	164(19)	0.0815
ν_2	1699	704(81)	468(54)	0.200
ν_3	1263	699(86)	465(57)	0.232
ν_4	790	563(82)	374(55)	0.263
$2\nu_2$	3372	38(6)	25(4)	0.033
d	2493	25(6)	17(4)	0.031
cis ν_1	3427	69(30)	23(10)	0.044
ν_2	1640	1250(240)	420(80)	0.272
ν_4	852	960(140)	322(47)	0.333
$2\nu_2$	3257	30(5)	10.1(1.7)	0.030

a This column gives the band strength ignoring the partition of the total HONO pressure between the two tautomers.

b 1 debye = 3.34×10^{-30} mC.

c The uncertainties in the last digits are given in parentheses.

d The assignment of this band is uncertain; it may be $\nu_2 + \nu_4$ or $2\nu_3$. We also cannot rule out the possibility this band belongs to cis-HONO.

standard deviation from the spread in the measurements, the estimated uncertainties in the equilibrium constants, and uncertainties in the temperature and pressure measurements. The uncertainty in the equilibrium constant for the formation of HONO, Eq. (8), is a major contributor to the uncertainties in the intensities. The major factors contributing systematic errors will be (a) the instrumental distortion of the intensity measurement due to incomplete resolution or due to non-linearities in the instrumental response function and (b) inaccuracies in the equilibrium constants under our experimental conditions, particularly due to the N_2 pressure needed to pressure-broaden the spectra.

Acknowledgement—This work was partially supported by the NASA Office of Upper Atmospheric Research.

REFERENCES

1. E. W. Kaiser and C. H. Wu, *J. Phys. Chem.* **81**, 1701 (1977).
2. W. H. Chan, R. J. Nordstrom, J. G. Calvert, and J. H. Shaw, *Chem. Phys. Lett.* **37**, 441 (1976).
3. L. H. Jones, R. M. Badger, and G. E. Moore, *J. Chem. Phys.* **19**, 1599 (1951).
4. G. E. McGraw, D. L. Bernitt, and I. C. Hisatsune, *J. Chem. Phys.* **45**, 1392 (1966).
5. R. Varma and R. F. Curl, *J. Phys. Chem.* **80**, 402 (1976).
6. M. Allegrini, J. W. C. Johns, A. R. W. McKellar, and P. Pinson, *J. Molec. Spectrosc.* **79**, 446 (1980).
7. A. G. Maki and R. L. Sams, to be published.
8. K. Narahari Rao, *Molecular Spectroscopy: Modern Research*, Vol. II. Academic Press, New York (1976).
9. V. M. Devi, P. P. Das, A. Bano, K. N. Rao, *J. Molec. Spectrosc.* **87**, 578 (1981).
10. L. G. Wayne and D. M. Yost, *J. Chem. Phys.* **19**, 41 (1951).
11. P. G. Ashmore and B. J. Tyler, *J. Chem. Soc.* 1017 (1961).
12. D. M. Waldorf and A. L. Babb, *J. Chem. Phys.* **39**, 432 (1963); **40**, 1165 (1964).
13. L. Harris and K. L. Churney, *J. Chem. Phys.* **47**, 1703 (1967).
14. W. R. Forsythe and W. F. Giauque, *J. Am. Chem. Soc.* **64**, 48 (1942).
15. I. R. Beattie and S. W. Bell, *J. Chem. Soc.* 1681 (1957).